IEEE Open Journal of
Intelligent Transportation
Systems

Received 4 August 2023; revised 31 October 2023 and 29 November 2023; accepted 30 November 2023. Date of publication 7 December 2023;
date of current version 29 December 2023.

Digital Object Identifier 10.1109/OJITS.2023.3340174

Fast Bidirectional Motion Planning for Self-Driving General N-Trailers Vehicle Maneuvering in Narrow Space

HANYANG ZHUANG[1] (Member, IEEE), QIYUE SHEN[2,3,4], YEQIANG QIAN[1] (Member, IEEE), WEI YUAN[1] (Member, IEEE), CHUNXIANG WANG[2,3,4] (Member, IEEE), AND MING YANG[2,3,4] (Member, IEEE)

[1]University of Michigan – Shanghai Jiao Tong University Joint Institute, Shanghai Jiao Tong University, Shanghai 200240, China
[2]Department of Automation, Shanghai Jiao Tong University, Shanghai 200240, China
[3]Key Laboratory of System Control and Information Processing, Ministry of Education of China, Shanghai Jiao Tong University, Shanghai 200240, China
[4]Shanghai Engineering Research Center of Intelligent Control and Management, Shanghai Jiao Tong University, Shanghai 200240, China

CORRESPONDING AUTHOR: M. YANG (e-mail: mingyang@sjtu.edu.cn)

This work was supported by the National Natural Science Foundation of China under Grant 62203294, Grant 62103261, Grant 62203301, and Grant 62173228.
This article has supplementary downloadable material available at https://doi.org/10.1109/OJITS.2023.3340174, provided by the authors.

ABSTRACT Self-driving General N-trailers (GNT) vehicles are one of the future solutions to build intelligent factory due to its flexibility and large load. Maneuvering of GNT vehicle to its destination requires accurate and robust motion planning. But the narrow operating environment causes nonlinear nonconvex constraints which are challenging. Furthermore, the nonholonomic constraints in GNT kinematics elevate the complexity in state space. Therefore, motion planning of GNT vehicle maneuvering in narrow space within a reasonable time and high success rate is a critical problem. This paper proposes a fast bidirectional motion planning algorithm to generate trajectories for GNT vehicles to maneuver in a narrow space. A coarse-to-fine motion planning paradigm has been proposed to balance the robustness and time. In the coarse step, an initial guess is generated through a bidirectional-sampled closed-loop Rapidly-exploring Random Tree, and a spatial-temporal safety corridor has been constructed to convert nonlinear nonconvex constraints to linear convex constraints. In the fine step, an optimal control problem is defined accordingly and solved to obtain feasible trajectory. Four different scenarios have been conducted with forward and reverse GNT vehicle maneuvering in a narrow environment. The results show that the proposed method outperforms state-of-the-art sampling-based and optimization-based motion planning methods.

INDEX TERMS Intelligent transportation system, tractor-trailer, motion planning, logistics.

I. INTRODUCTION

SELF-DRIVING tractor-trailer vehicle refers to a system composed of one or more trailers driven by a self-driving tractor. Tractor-trailer vehicles have strong loading capability, therefore, have been widely used in freight transportation. This paper mainly focuses on the low-speed transportation scenarios in factories and docks that running slower than 5 m/s, rather than high-way truck-trailer vehicles. Low-speed operating condition reliefs the vehicle from dealing with dynamic behavior at high-speed, but the environment in such conditions is significantly complicated than high-way road. The narrow driving spaces limit the free maneuvering of self-driving tractor-trailer vehicle, especially when the vehicle is approaching destination or parking. It is a hard task for experienced human drivers [1], and even more challenging for motion planning of the self-driving tractor-trailer system.

Motion planning aims at generating a kinematically feasible trajectory with the information of vehicle's location [2] and surrounding objects [3], [4], [5]. This trajectory will then be used to control the vehicle [6]. Extensive researches have been conducted for vehicles and robots using searching-based [7], [8], [9], [10],

The review of this article was arranged by Associate Editor Xin Xia.

sampling-based [11], optimization-based [12], [13], [14], [15], spline-based [16], [17], tree-based [18], and deep learning-based [19] approaches, etc. Conventional vehicles running on express road or highway require smooth planning [20], [21] and safe control [22], [23]. However, compared to conventional vehicles, tractor-trailer vehicles have higher dimensions in state space and nonholonomic constraints, which means the kinematic model of tractor-trailer vehicles is more complex. Moreover, the narrow space in environment which introduces additional nonlinear and nonconvex constraints. It raises significant challenges for motion planning algorithms to find feasible solutions.

The motion planning of tractor-trailer vehicle maneuvering in narrow spaces requires the generated trajectory to be kinematically feasible and collision-free. Also, the driving direction can be forward and reversed, so the planner should be compatible with both moving directions. Moreover, even though the time consumption of planning is not essential, it should be at the magnitude of seconds for real application.

To focus on the motion planning of tractor-trailer vehicles, extensive researches have been carried out [24], [25], [26]. A hybrid A*-based method was utilized by Thakkar et al. for tractors with semi-trailer path planning [27]. Ljungqvist et al. [28] presented their work using a state lattice motion planner. Some works generalize RRT to generate a kinematically feasible path that can be followed by a specific controller [29], [30]. This closed-loop controller paradigm to connect points has been verified [31], [32], [33]. All these methods depend on the scale of motion primitives or sampling steps. Too large of the scale leads to failure of planning, while too small of the scale causes low computing efficiency. Ghilardelli et al. adopted splines to realize finer tractor-trailer motion planning considering kinematic model constraints [34], without considering narrow spaces.

Further investigations using optimization-based approach works with aforementioned sampling-based or searching-based methods can achieve better performance [35]. Oliveria et al. designed a path planning algorithm in Frenet coordinate with various cost functions and collision constraints by solving nonlinear optimization problem [36], [37]. However, the method takes significant computing time. Li et al. [38], [39] and Cen et al. [40] extending optimization-based methods to solve the parking motion planning problem of tractor-trailer vehicles.

As a short summary, state-of-the-art tractor-trailer motion planning methods usually combine the multiple methods together. A searching-based or sampling-based method is used in the first stage to find an initial guess. Then an optimization-based method is initiated along the initial guess, to generate the trajectory. This two-stage coarse-to-fine paradigm is reasonable for such a complex kinematic system in constrained environments. The main pain point is the balance of significant time cost of high accuracy initial guess generation and low availability with a low-quality initial guess. Therefore, this paper will mainly focus on improving the motion planning computing efficiency.

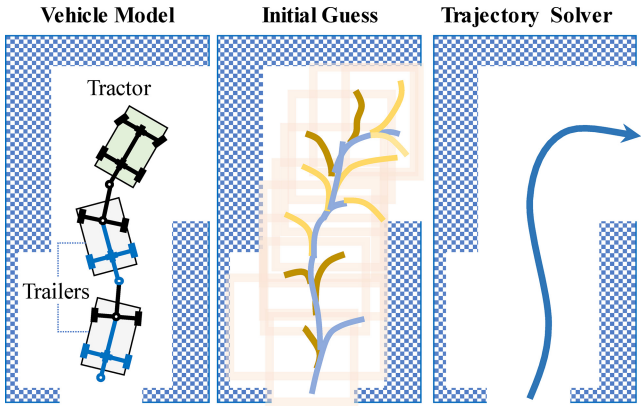

FIGURE 1. The coarse-to-fine paradigm of GNT motion planning.

Furthermore, many of the motion planning algorithms only apply for single direction movement, i.e., either forward only or reverse only. So, the minor target of this paper is to enable the motion planning for both directions.

General N-trailers (GNT) vehicle [41] as one type of tractor-trailer system is commonly used in reality and will be focused in this paper. In the operating of GNT vehicles, the strict constraints of the narrow environment space lead to a limited feasible solution. This paper first utilizes a bidirectional closed-loop random rapidly-exploring random tree (RRT) to link the origin and destination so that a quick but coarse initial guess for both moving directions can be established. Only with an initial guess is not enough since the downstream optimization process rely on solving high-dimensional nonlinear nonconvex problems, which may fail to find a feasible solution. Therefore, the temporal-spatial safety corridor [42], [43] idea for unmanned aerial vehicle will be applied to convert nonlinear nonconvex constraints to linear convex ones to benefit the optimization solver. Optimization-based motion planning method is then adopted based on these constraints to find the trajectory. Therefore, the main contribution of this paper is twofold:

1) A motion planning algorithm for GNT vehicle maneuvering in forward and reverse directions in narrow spaces has been proposed and verified.
2) A time-efficient linear safety constraints generation approach using bidirectional closed-loop RRT and spatial-temporal safety corridor has been proposed.

The rest of this paper is organized as follows. In Section II, the kinematic model of the GNT vehicles is conducted. In Section III, the methodology of the research is described, and the pipeline of the proposed planning algorithm is explained. In Section IV, the results in the simulation environment are depicted and the discussion of the results is provided. Finally, the conclusion of this paper is summarized in Section V.

II. VEHICLE MODEL

The GNT vehicle studied in this paper is illustrated in Fig. 2, which is commonly adopted in the logistics of factories, airports, and docks. According to current research [44],

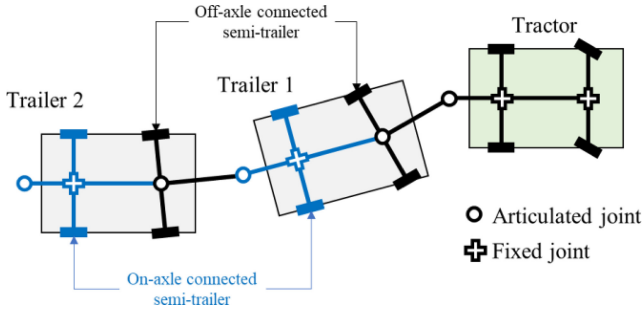

FIGURE 2. Illustration of GNT vehicle studied in this paper.

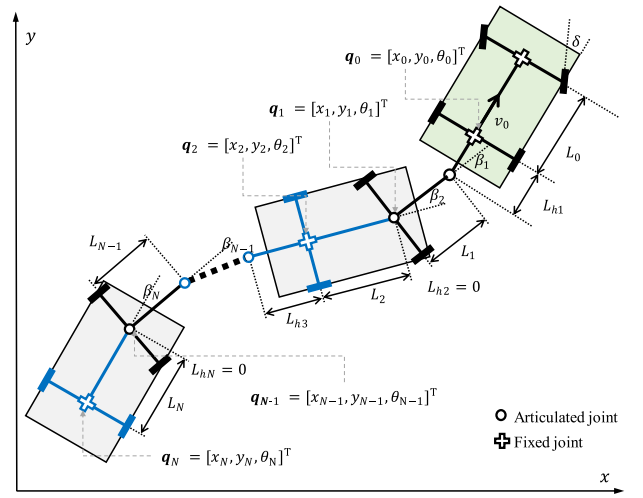

FIGURE 3. Kinematic model of GNT vehicle.

each full-trailer in a GNT vehicle can be decomposed into an on-axle connected semi-trailer (rear axle) to an off-axle connected semi-trailer (front axle) inside this full-trailer.

The scope of this paper focuses on the low-speed operating scenarios for campus or factory logistics, so the driving speed of the vehicle is assumed to be lower than 5m/s. In this operating condition, the tire force and sideslipping of GNT vehicles can be neglected according to previous research [45]. Therefore, it is reasonable to use a kinematic model to describe a GNT vehicle in parking scenarios [36]. According to Fig. 3, each full-trailer consists of two parts; therefore, N full-trailers will lead to $2N$ semi-trailers (called "bodies"). In the following derivations, $i \in [0,\ 2N]$ indicates the index of the semi-trailer inside the full-trailer. The tractor's rear axle has an index of i=0, which is also a body.

For each body the state variable of each body is described as follows:

$$\boldsymbol{q_i} = \begin{bmatrix} \theta_i \\ x_i \\ y_i \end{bmatrix} \tag{1}$$

where θ_i is the yaw angle of body i; x_i and y_i indicate the location of body i in cartesian coordinates.

The control variable of each body is represented as:

$$\boldsymbol{u_i} = \begin{bmatrix} \omega_i \\ v_i \end{bmatrix} = \begin{bmatrix} \dot{\theta}_i \\ v_i \end{bmatrix} \tag{2}$$

where v_i is the linear velocity; ω_i is the angular velocity which is the derivative of the yaw angle.

The kinematics of each body, following relationship, keeps consistent:

$$\dot{x}_i \sin\theta_i - \dot{y}_i \cos\theta_i = 0 \tag{3}$$

The combination of (1) and (3) lead to the rate of state variable change:

$$\dot{\boldsymbol{q}}_i = \begin{bmatrix} \dot{\theta}_i \\ \dot{x}_i \\ \dot{y}_i \end{bmatrix} = \begin{bmatrix} 1 & 0 \\ 0 & \cos\theta_i \\ 0 & \sin\theta_i \end{bmatrix} \begin{bmatrix} \omega_i \\ v_i \end{bmatrix} = \boldsymbol{G}(\boldsymbol{q_i})\boldsymbol{u_i} \tag{4}$$

where $\boldsymbol{G}(\boldsymbol{q_i})$ describes how the control variable acts on the state variable of body i. Moreover, the control variables of adjacent bodies are not independent [46]. The transfer matrix of control variables of adjacent bodies follows:

$$\boldsymbol{u_i} = \begin{bmatrix} -\frac{L_{\text{hi}}}{L_i}\cos\beta_i & \frac{1}{L_i}\sin\beta_i \\ L_{\text{hi}}\sin\beta_i & \cos\beta_i \end{bmatrix} \boldsymbol{u_{i-1}} = \boldsymbol{J_i}(\boldsymbol{\beta_i})\boldsymbol{u_{i-1}} \tag{5}$$

where L_i is the wheelbase of body i; L_{hi} is the distance of off-axle connection of body i; $\boldsymbol{J}_i$ is the transfer matrix that is invertible when $L_{hi} \neq 0$.

The state variable of the entire GNT vehicle can be uniquely described by the configuration of the tractor state and the joint angles of all trailers, as follows:

$$\boldsymbol{q} = \begin{bmatrix} \beta_1 & \dots & \beta_{2N} & \theta_0 & x_0 & y_0 \end{bmatrix}^T = \begin{bmatrix} \boldsymbol{\beta} \\ \boldsymbol{q_0} \end{bmatrix} \tag{6}$$

where $\boldsymbol{\beta}$ is the vector of joint angles indicating the yaw angle of each body to its preceding body, $\beta_i = \theta_{i-1} - \theta_i$.

Equation (6) describes the GNT vehicle starting from the tractor; however, this equation also stands starting from any vehicle body. In this situation, only $\boldsymbol{q}_0$ will be replaced by the state of the first body, and the total trailer number N will be reduced accordingly. So, the reduction of the following relation leads to the kinematic model of the GNT vehicle with the following form:

$$\dot{\boldsymbol{q}} = \begin{bmatrix} \dot{\boldsymbol{\beta}} \\ \dot{\boldsymbol{q}}_j \end{bmatrix} = \begin{bmatrix} \boldsymbol{S_\beta}(\boldsymbol{\beta}) \\ \boldsymbol{S_j}(\boldsymbol{\beta}, \boldsymbol{q_j}) \end{bmatrix} \boldsymbol{u_0} \tag{7}$$

where $\boldsymbol{S}_\beta$ is the transfer matrix of joint-angle between adjacent bodies; $\boldsymbol{S}_j$ is the transfer matrix of state variable between adjacent bodies. They have the form as follows:

$$\boldsymbol{S_\beta}(\boldsymbol{\beta}) = \begin{bmatrix} \boldsymbol{c}^T\boldsymbol{\Gamma_1}(\beta_1) \\ \boldsymbol{c}^T\boldsymbol{\Gamma_2}(\beta_2)\boldsymbol{J_1}(\beta_1) \\ \vdots \\ \boldsymbol{c}^T\boldsymbol{\Gamma}_N(\boldsymbol{\beta}_N)\boldsymbol{J}^{\boldsymbol{1}}_{N-1}(\boldsymbol{\beta}) \end{bmatrix} \tag{8}$$

$$\boldsymbol{S_j}(\boldsymbol{\beta}, \boldsymbol{q_j}) = \begin{bmatrix} \boldsymbol{d}^T\boldsymbol{J}^{\boldsymbol{1}}_{\boldsymbol{j}}(\boldsymbol{\beta}) \\ \boldsymbol{d}^T\boldsymbol{J}^{\boldsymbol{1}}_{\boldsymbol{j}}(\boldsymbol{\beta})\cos\theta_j \\ \boldsymbol{d}^T\boldsymbol{J}^{\boldsymbol{1}}_{\boldsymbol{j}}(\boldsymbol{\beta})\sin\theta_j \end{bmatrix} \tag{9}$$

where $\boldsymbol{J}^{\boldsymbol{1}}_{\boldsymbol{j}}(\boldsymbol{\beta}) = \boldsymbol{J}_j(\beta_j)\boldsymbol{J}_{j-1}(\beta_{j-1})\cdots\boldsymbol{J}_1(\beta_1)$ and $\boldsymbol{\Gamma}_i(\beta_i) = \boldsymbol{I} - \boldsymbol{J}_i(\beta_i)$; $\boldsymbol{c}^T = \begin{bmatrix} 1 & 0 \end{bmatrix}$ and $\boldsymbol{d}^T = \begin{bmatrix} 0 & 1 \end{bmatrix}$.

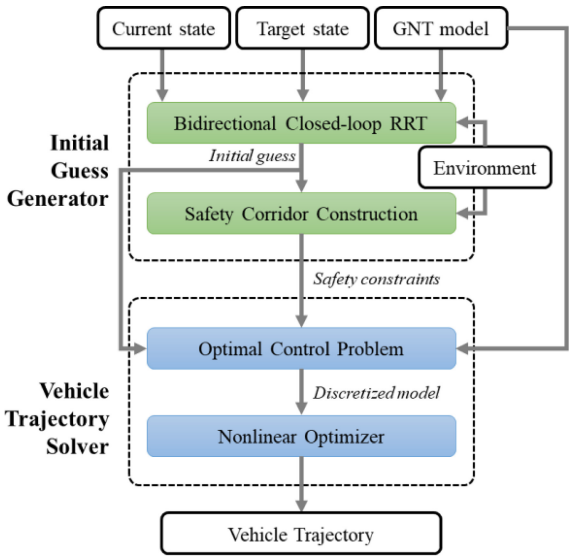

FIGURE 4. Framework of the proposed method.

In this GNT vehicle, any adjacent full-trailers, or the tractor and first full-trailer, can be represented by a G2T model, i.e., a "tractor" with a full-trailer (modeled by two semi-trailers). This "tractor" can be the actual tractor at the front or the preceding full-trailer whose state can be derived by conducting the kinematic model sequentially from the beginning. Therefore, this paper further extracts the G2T system to illustrate the kinematic model better:

$$\begin{cases} \dot{\beta}_1 = v_0\left(\frac{\tan\delta}{L_0} - \frac{\sin\beta_1}{L_1} + \frac{L_{h1}\cos\beta_1\tan\delta}{L_0L_1}\right) \\ \dot{\beta}_2 = v_0\left(\frac{\sin\beta_1}{L_1} - \frac{\cos\beta_1\sin\beta_2}{L_2} - \frac{L_{h1}\cos\beta_1\tan\delta}{L_0L_1} - \frac{L_{h1}\sin\beta_1\tan\delta}{L_0L_2}\right) \\ \dot{x}_0 = v_0\cos\theta_0 \\ \dot{y}_0 = v_0\sin\theta_0 \\ \dot{\theta}_0 = v_0\frac{\tan\delta}{L_0} \end{cases} \tag{10}$$

where δ is the front wheel angle of the tractor; $L_{h2} = 0$ in this configuration due to on-axle connection.

III. MOTION PLANNING ALGORITHM

A. ALGORITHM PIPELINE

The planning algorithm of GNT vehicle maneuvering consists of two steps: The first step is to construct the initial guess. In this step, a bidirectional closed-loop RRT is proposed to get the initial guess, and a safety corridor along the initial guess is generated.

The second step is to generate the trajectory. The planning problem is modeled as a discretized nonlinear optimization problem. The safety corridor is then used in this paper to convert nonconvex nonlinear constraints to convex linear constraints. Ultimately, the GNT vehicle maneuvering motion planning is completed by solving the nonlinear optimization problem.

B. INITIAL GUESS GENERATOR

The closed-loop RRT has been proposed by multiple researchers in their previous work [15], [16]. It works well in forwarding motion; however, the vehicle's reverse motion's instability makes it difficult to plan the path to the destination [31], [32]. However, the closed-loop controller used in such a method may not fulfill the kinematic constraints, and the sampling process takes too much time to generate a full path. Therefore, a bidirectional closed-loop RRT is proposed to ensure the vehicle can park at the correct location and attitude. Moreover, this approach will be compatible with forward and reverse maneuvering motion planning.

Algorithm 1 Bidirectional Sampling

Input:
Initial location $\boldsymbol{p}_0(\boldsymbol{x}_0, \boldsymbol{y}_0)$
Target location $\boldsymbol{p}_g(\boldsymbol{x}_g, \boldsymbol{y}_g)$
Fixed velocity $\boldsymbol{v}_0$
Output:
A vector of path points:$\{(\boldsymbol{x}_i, \boldsymbol{y}_i)\}$
Function:
while iteration is less than max number
RRT to obtain $\boldsymbol{p_1}(\boldsymbol{x}_1, \boldsymbol{y}_1)$ in forward direction
RRT to obtain $\boldsymbol{p}_{g-1}(\boldsymbol{x}_{g-1}, \boldsymbol{y}_{g-1})$ in reverse direction
calculate control variable $\boldsymbol{u}_1$ from $\boldsymbol{p}_0$ to $\boldsymbol{p}_1$ using pure pursuit
calculate control variable $\boldsymbol{u}_{g-1}$ from $\boldsymbol{p}_g$ to $\boldsymbol{p}_{g-1}$ using pure pursuit
save $\boldsymbol{p}_1$, $\boldsymbol{p}_{g-1}$, $\boldsymbol{u}_1$, $\boldsymbol{u}_{g-1}$ every Δt in vector
  if two paths are connectable
connect the two paths
calculate the cost and save vector
  end if
end while
export the vector with minimal cost
end Function

In order to sample in reverse motion, a forward GNT vehicle motion in a negative time step is utilized to build the path. The invertibility of the GNT kinematic model in the time domain has been proven [30]. The path of forward sampling in negative time leads to a path of reverse sampling. The algorithm is developed by maintaining two tree structures; one starts from the start location and the other starts from the target location. The closed-loop controller is a pure pursuit controller to accelerate the bidirectional sampling process since the accuracy requirement is not strict.

The connectable of forward and reverse sampling is shown in Fig. 5. The exact equality of all bodies' states in both forward and reverse sampling is complicated to reach and may take extremely long. Since this paper only uses the result as an initial guess to construct a spatial-temporal safety corridor, the connectable condition is checked by drawing circles of the axle of each body. If all the corresponding circles of the two sampling paths have overlapped, then this condition is considered as these two sampling paths are connectable.

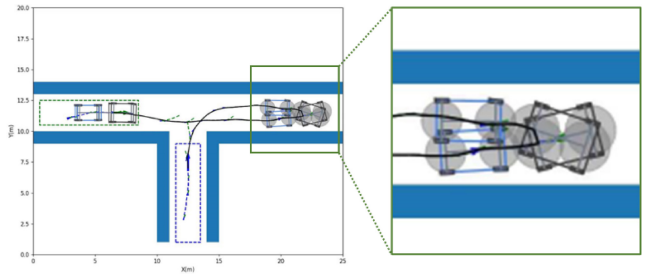

FIGURE 5. Illustration of connectable condition.

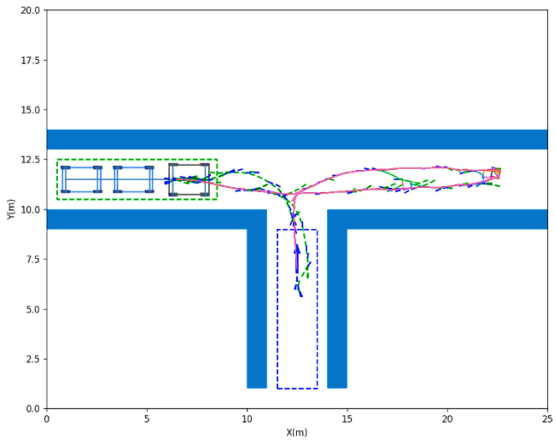

FIGURE 6. An initial guess obtained by bidirectional sampling.

As depicted in Fig. 6, the initial guess using the bidirectional sampling method is obtained. The green path indicates the forward sampling process, and the blue path indicates the reverse sampling process. The pink line indicates an initial guess using this method. Furthermore, a heuristic approach is also adopted to improve the success rate of path planning and accelerate the convergence speed. During the RRT of forward sampling, the points in reverse sampling tree are used as heuristic items. During the RRT of reverse sampling, the points in the forward sampling tree are used as heuristic items.

The algorithm may generate multiple initial guesses; therefore, a cost function will be used to evaluate them and obtain the optimal. This paper proposed a cost function of three parts: safety cost, length cost, and smoothness cost.

Safety cost, noted by cost $_{\text{safety}}$, is calculated in a grid map of the environment. In each time step Δt, a circle with safety radius (r_s) is drawn with the center of each path point. The area of grids occupied by these circles is noted by M. Within this area, any grid also occupied by obstacles is summed up to obtain the area noted by N, where $N \leq M$. M and N are then used to calculate the cost by (11). Value K is the number of sampling periods from the beginning to the timing of the current sampling result. This cost indicates that the generated path should tend to keep obstacles away from the path. However, the cost is infinite if the vehicle collides with any obstacle. Preventing collision has the highest priority so that any trajectory that has potential collision should not be taken into consideration. The infinite value shown in (11) indicates that if a potential trajectory has collision with environment, the costs will be set to maximum and be discarded later. Its implementation is to use a super large value to represent infinity, and it cannot add or subtract to other cost values. The collision is checked by putting the vehicle geometry at the sampled state to see if there is any overlap between GNT vehicle geometry and any obstacle.

$$\text{cost}_{\text{safety}} = \begin{cases} (\Sigma_{i=1}^{K} e^{N_i/M_i})/K, & \text{no collision} \\ \infty, & \text{collided} \end{cases} \tag{11}$$

Length cost, noted by $\text{cost}_{\text{length}}$, indicates the length of the generated path, which is calculated by the following:

$$\text{cost}_{\text{length}} = \Sigma_{i=1}^{K-1} \sqrt{(x_{i+1} - x_i)^2 + (y_{i+1} - y_i)^2} \tag{12}$$

Smoothness cost, noted by $\text{cost}_{\text{smooth}}$, indicates that the tractor front wheel angle and front wheel angular velocity should be smaller to reduce the lateral action of the GNT vehicle. Therefore, this cost is calculated as follows:

$$\text{cost}_{\text{smooth}} = w_\delta \text{cost}_\delta + w_{\Delta\delta} \text{cost}_{\Delta\delta} \tag{13}$$

where w_δ and $w_{\Delta\delta}$ represent the weights of the front wheel angle and front wheel angular velocity cost, respectively. They are presented by:

$$\begin{cases} \text{cost}_\delta = (\Sigma_{i=1}^{K} e^{\frac{|\delta(i)|}{|\delta_{\max}|}})/K \\ \text{cost}_{\Delta\delta} = (\Sigma_{i=2}^{K} e^{\frac{|\dot{\delta}(i)|}{|\dot{\delta}_{\max}|}})/(K-1) \end{cases} \tag{14}$$

where $\delta(i)$ is the front wheel angle at i step; $\dot{\delta}(i)$ is the front wheel angular velocity at i step; $\delta_{\max}$ and $\dot{\delta}_{\max}$ are the maximum value of δ and $\dot{\delta}$. At last, all the cost components are added together to the following form:

$$\text{cost} = w_1 \text{cost}_{\text{safety}} + w_2 \text{cost}_{\text{length}} + w_3 \text{cost}_{\text{smooth}} \tag{15}$$

C. VEHICLE TRAJECTORY SOLVER

Obtaining the initial guess is not feasible to drive; therefore, an optimal-control-based path planning algorithm is applied to the initial guess to ensure safety and optimality.

The state transition process of the self-driving vehicle to the destination from its initial location is the core of the path planning problem. So, it is reasonable to model the path planning process as a state transition process and solve it by the optimal control mechanism. The state transition process can be presented as:

$$\dot{\boldsymbol{x}}(t) = f(\boldsymbol{x}(t), \boldsymbol{u}(t)) \tag{16}$$

where $\boldsymbol{x}$ indicates the state of the tractor-trailer vehicle, with an initial state of $\boldsymbol{x}(0) = \boldsymbol{x}_0$, and $\boldsymbol{u}(t)$ is the control input. The optimal control problem is then illustrated as:

$$\min_{u} \int_0^{t_f} \Gamma(\boldsymbol{x}(t), \boldsymbol{u}(t))\text{dt} + \Phi(\boldsymbol{x}(t_f), \boldsymbol{X}_{goal})$$

$$\text{s. t.} \quad \begin{cases} \dot{\boldsymbol{x}}(t) = f(\boldsymbol{x}(t), \boldsymbol{u}(t)) \\ \boldsymbol{x}(0) = \boldsymbol{x}_0 \\ \boldsymbol{x}(t_f) = \boldsymbol{X}_{goal} \\ \boldsymbol{x}(t_f) \in \boldsymbol{X}_{free}(t) \\ u(t) \in U \end{cases} \tag{17}$$

where Γ indicates the cost function of vehicle movement; Φ indicates the cost function of final state at the goal; $\boldsymbol{X}_{\text{free}}(t)$ is the set of all non-collision states; $\boldsymbol{X}_{\text{goal}}$ is the constraint of target state; t_f is the final time to arrival; $\boldsymbol{U}$ is the control input to be solved.

For a path planning problem, the cost function of vehicle movement Γ includes the state and control variables:

$$\begin{aligned} \Gamma(\boldsymbol{x}(t), \boldsymbol{u}(t)) = w_1 &\left(\frac{\delta(t+\Delta t) - \delta(t)}{\Delta t} \right)^2 \\ &+ w_2 \left(\frac{v_0(t+\Delta t) - v_0(t)}{\Delta t} \right)^2 \\ &+ \sum_{i=1}^{M} w_3 \left(\frac{\beta_i(t+\Delta t) - \beta_i(t)}{\Delta t} \right)^2 \end{aligned} \tag{18}$$

where M indicates the number of trailers. Furthermore, the cost function of the final state Φ is described by the time:

$$\Phi\big(\boldsymbol{x}(t_f), \boldsymbol{X}_{goal}\big) = t_f \tag{19}$$

The state transition process in the constraints can be replaced by the vehicle model in (10), and the constraint of the target state is set to be the location of the destination by:

$$\boldsymbol{x}(t_f) = \boldsymbol{X}_{goal} \tag{20}$$

The safety constraint indicated by $\boldsymbol{x}(t_f) \in \boldsymbol{X}_{free}(t)$ represents all the spaces where the vehicle is safe, and movement is collision-free. The current method uses a triangle-area-based criterion to generate this safety zone [14]. Nevertheless, this constraint is highly nonlinear and non-convex, which is a challenge for the solver to converge within a short time. Consequently, this paper proposes an approach to construct a spatial-temporal safety corridor to simplify this safety constraint, inspired by unmanned aerial vehicles' work [42]. The safety corridor provides a set of linear inequality constraints along various timing, instead of modeling the environment as a large nonconvex constraint. With the help of safety corridor construction, the optimization process will be easier to converge. The safety corridor is constructed by expanding from each vehicle state in the initial guess. The construction process ends when the next expansion intersects with static obstacles such as walls or pillars. The corridor construction method and the result are presented in Fig. 7.

Here the definition of all the constraints shown in (17) is obtained. The Multi-shooting method [47] discretizes the control and state variables. The optimal control problem is then converted to a nonlinear optimization problem, as depicted below:

$$\min_{x,u} \sum_{k=0}^{N-1} \Gamma(\boldsymbol{x}_k, \boldsymbol{u}_k) + \Phi(\boldsymbol{x}, \boldsymbol{t})$$

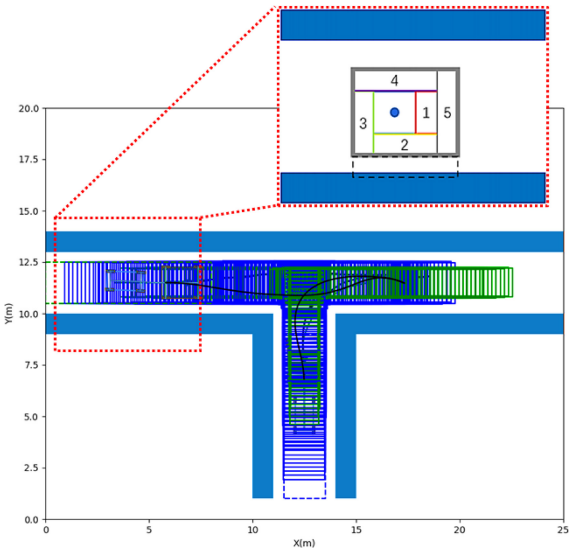

FIGURE 7. The result of spatial-temporal safety corridor. Green boxes indicate the corridor for tractors, and blue boxes indicate the corridor for trailers.

$$\text{s. t.} \quad \begin{cases} \boldsymbol{x}_{k+1} = f(\boldsymbol{x}_k, \boldsymbol{u}_k)dt + \boldsymbol{x}_k \\ \boldsymbol{x}_0 = \boldsymbol{q}_0 \\ \boldsymbol{x}_N = \boldsymbol{q}_{\text{goal}} \\ \boldsymbol{x}_k \in \boldsymbol{S}_k \\ \boldsymbol{u}_k \in \boldsymbol{U}_k \end{cases} \tag{21}$$

where $f(\boldsymbol{x}_k, \boldsymbol{u}_k)$ is the vehicle kinematic model in discrete mode; $\boldsymbol{S}_k$ indicates the k-th safety corridor, and $\boldsymbol{U}_k$ indicates the k-th control constraint of the max steer rate and acceleration. The converted optimization problem is then solved by IPOPT [48].

IV. SIMULATION RESULTS AND DISCUSSIONS

A. SIMULATION PLATFORM

The proposed method is validated through simulation. The simulation platform is developed in Python. The framework of the simulation platform is depicted in Fig. 8. A map module is used to set the static obstacles in the environment to enable interaction between the vehicle and the environment. The planning module is used to generate the path, and the control module is used to implement the optimal control module. The discrete vehicle model, as derived above, is utilized to generate state variables in the next time step with the control variables at the current step. Noises are added to the position and yaw. The platform is running on an x86 computer with Intel Core i7-10510U@1.80GHz.

B. TEST SCENARIOS

Two different scenarios are used in this investigation, i.e., a vertical and a parallel scenario. Since the maneuvering process usually takes place at the end of the transportation task, the distance to park does not need to be very long, so the scenarios are constructed within a 20m×20m area. The two scenarios have very limited spaces for vehicles to maneuver. The solid blue pixels indicate the environment constraints formed by walls or assigned by safety areas. In each scenario,

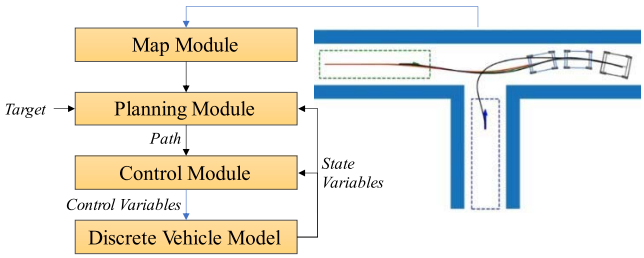

FIGURE 8. The framework of the simulation platform.

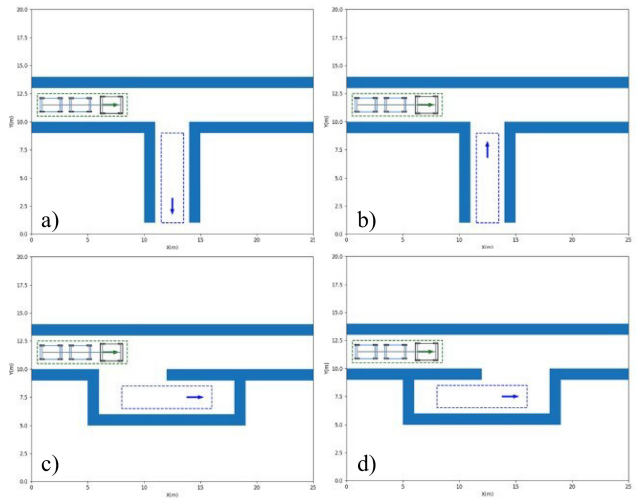

FIGURE 9. The scenarios and test cases.

there are two test cases that in one of them the vehicle drives forward to the target position (Fig. 9 a) and c)), while in the other one, the vehicle drives back to the target position (Fig. 9 b) and d)).

C. BIDIRECTIONAL SAMPLING RESULTS

This part presents the possible results generated through the bidirectional sampling process. It is easy to identify that there might be multiple possible sampling solutions. The green lines indicate the sampling result when vehicle moves forward, and the blue lines are the reverse sampling result. Multiple sampling results come from the randomness of the RRT process; therefore, the evaluation process through the cost function of (15) is necessary. The path with the lowest cost is presented in the black line and will be considered the initial guess. It is also easy to see that most results are not feasible to drive with substantial discontinuous corners. A further optimization process is required to generate the path to drive.

D. SAFETY CORRIDOR CONSTRUCTION RESULTS

The safety corridor is constructed according to the initial guess. It provides constraints for the optimization process. Moreover, the threshold of collision avoidance can be tuned through the size of the corridor construction process. The green boxes indicate the tractor's corridor; the blue and yellow boxes indicate that of the first and second trailers, respectively.

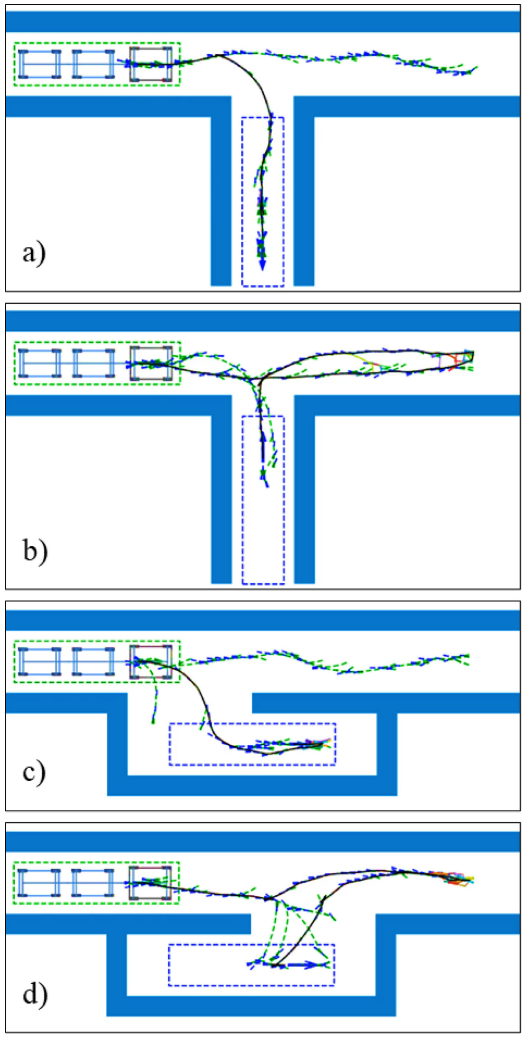

FIGURE 10. Bidirectional sampling results. a) Forward vertical scenario; b) Reverse vertical scenario; c) Forward parallel scenario; d) Reverse parallel scenario.

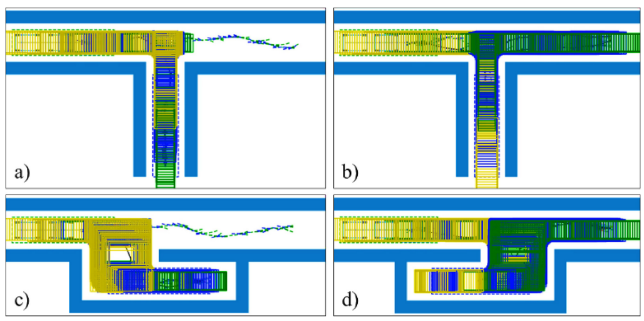

FIGURE 11. Safety corridor construction results. a) Forward vertical scenario; b) Reverse vertical scenario; c) Forward parallel scenario; d) Reverse parallel scenario.

E. MOTION PLANNING RESULTS

The optimal control problem can be constructed and solved with the initial guess and safety corridor. This result leads

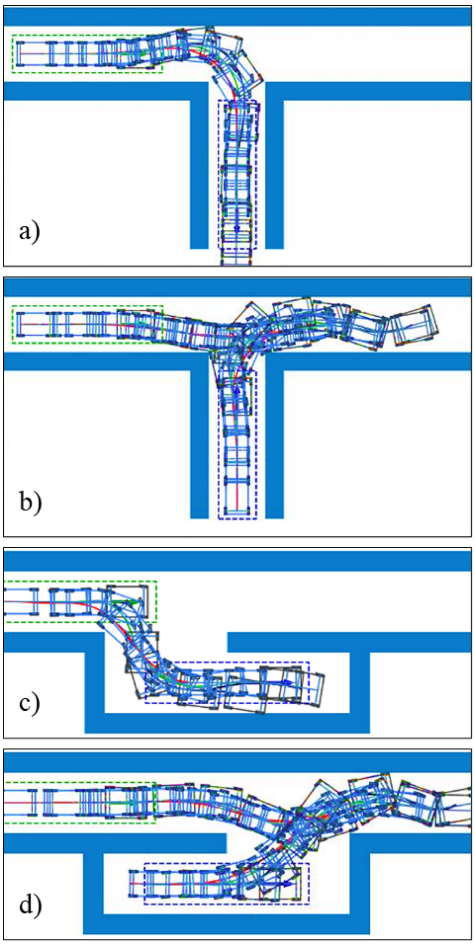

FIGURE 12. Optimal control results. a) Forward vertical scenario; b) Reverse vertical scenario; c) Forward parallel scenario; d) Reverse parallel scenario.

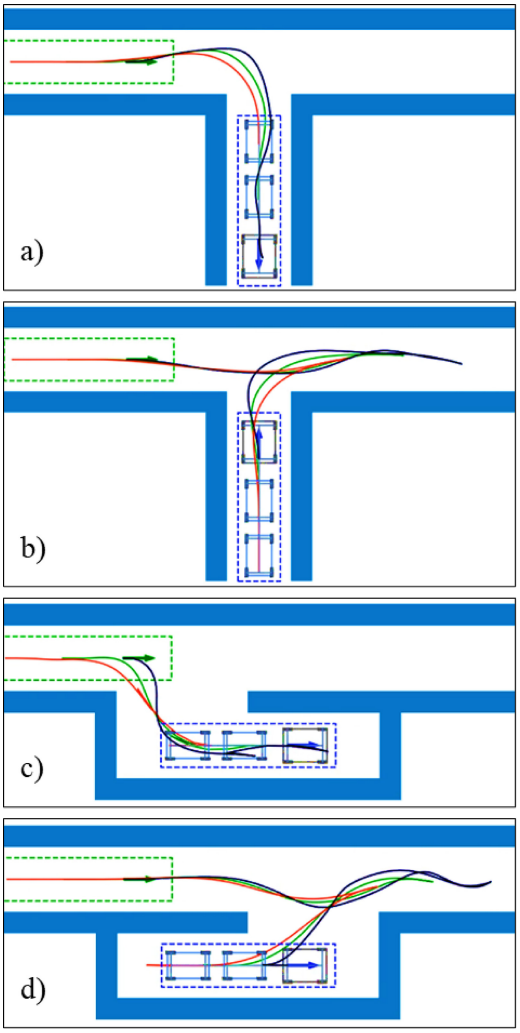

FIGURE 13. Path planning results. a) Forward vertical scenario; b) Reverse vertical scenario; c) Forward parallel scenario; d) Reverse parallel scenario.

to a series of vehicle states along the optimal path. The illustration of the vehicle states at each point can be found in Fig. 12. A smooth and safe path for the G2T vehicle in such a narrow space can be generated. There is no collision with the static obstacles. The safety margin seems small in this case because the optimal solutions during the optimal control process are always found near the boundary of constraints. The expansion's size while constructing the safety corridor can be increased to maintain further safety distance.

The path of the tractor and each trailer can be found in Fig. 13. In all cases, the planning algorithm can generate a feasible solution to fulfill the requirement of maneuvering to the target box.

The results have demonstrated the capability of the proposed mechanism for successful path planning in narrow spaces with forward and reverse movements. Any feasible solution to the correct destination with the expected final state would be enough. However, due to the limitation in space and high-order vehicle models, the time cost for planning is of the essence. Even though most of the planning methods can eventually achieve a result, the time cost is unacceptable due to the complexity of the model and environment.

Some quantitative comparisons are made to two other commonly used methods; one is HASC [40] with Hybrid A* as an initial guess. The initial guess is then used to generate the corridor, as illustrated in this paper. Then the HASC method was adopted within the constraint formed by the corridor. The other comparison experiment was carried out using OMPCT [39]. Both a tractor with one trailer and two trailers are used for testing. The least time costs of these two methods and the proposed method for multiple runs are summarized in the following tables:

In the forward scenario test cases, planning time greater than 30 s is considered unacceptable, while this value is set to 60 s for reverse scenario. Furthermore, N/A indicates that the solver cannot get a solution.

In the result of TABLE 1, the OMPCT shows the best performance in planning a feasible solution in the forward vertical scenario. The proposed method takes slightly more time to find the solution. The HASC method takes the longest time. The results become different in reverse vertical scenario as shown in TABLE 2. The HASC can generate the solution

TABLE 1. Forward vertical scenario.

	HASC (s)	**OMPCT** (s)	**Proposed method** (s)
1 trailer	19.29	**2.18**	3.09
2 trailers	> 30	**3.93**	4.85

TABLE 2. Reverse vertical scenario.

	HASC (s)	**OMPCT** (s)	**Proposed method** (s)
1 trailer	> 60	N/A	**2.49**
2 trailers	> 60	N/A	**5.28**

TABLE 3. Forward parallel scenario.

	HASC (s)	**OMPCT** (s)	**Proposed method** (s)
1 trailer	4.42	**0.87**	1.32
2 trailers	10.12	**1.90**	2.25

TABLE 4. Reverse parallel scenario.

	HASC (s)	**OMPCT** (s)	**Proposed method** (s)
1 trailer	> 60	N/A	**1.25**
2 trailers	> 60	N/A	**2.47**

after a long time, while the OMPCT method fails to search for the solution. The proposed method takes a few seconds to plan the trajectories for both one trailer and two trailers configuration. This result indicates that the proposed method is compatible with motion planning for both forward and reverse man processes.

From TABLE 3 and 4, similar conclusions can be drawn that all these three methods are capable of motion planning in the forward parallel scenario within 10 seconds. The OMPCT generates the trajectory within minimal time; the proposed method takes longer; the HASC takes the longest time. While in the reverse parallel scenario, the HASC still takes a long time, and the OMPCT cannot find the solution. The proposed method takes about 2.5 seconds to generate a feasible solution for 2 trailers configuration.

V. CONCLUSION

This paper has proposed a maneuvering motion planning algorithm for self-driving general N-trailers (GNT) vehicles in narrow spaces. The contributions and main findings of this paper are as follows:

1) A motion planning algorithm for GNT vehicle maneuvering in forward and reverse directions in narrow spaces has been proposed and verified. A two-stage coarse-to-fine paradigm planning method has been proposed. A first sampling-based initial guess planner and an optimization-based planner are combined in this paper.
2) A time-efficient linear safety constraints generation approach using bidirectional closed-loop RRT and spatial-temporal safety corridor has been proposed. The safety corridor can convert the nonlinear nonconvex constraints into linear convex constraints. Therefore, the optimization-based planner can be easier to yield convergence.
3) A simulation platform has been developed, and the proposed motion planning algorithm has been validated and compared to two state-of-the-art methods. Four test cases of both forward and reverse maneuvering have demonstrated the capability of the proposed method. The successful planning results can be calculated in several seconds despite the movement direction and limitation of the spaces.

Further investigation will focus on developing the entire system for ground testing with integrating appropriate GNT vehicle controllers. The control precision of the GNT vehicle to follow the generated path is still a challenging issue.

REFERENCES

[1] B. Li, K. Wang, and Z. Shao, "Time-optimal trajectory planning for tractor-trailer vehicles via simultaneous dynamic optimization," in *Proc. IEEE/RSJ Int. Conf. Intell. Robots Syst. (IROS)*, 2015, pp. 3844–3849.

[2] X. Xia, N. P. Bhatt, A. Khajepour, and E. Hashemi, "Integrated inertial-LiDAR-based map matching localization for varying environments," *IEEE Trans. Intell. Veh.*, vol. 8, no. 10, pp. 4307–4318, Oct. 2023.

[3] Z. Meng, X. Xia, R. Xu, W. Liu, and J. Ma, "HYDRO-3D: Hybrid object detection and tracking for cooperative perception using 3D LiDAR," *IEEE Trans. Intell. Veh.*, vol. 8, no. 8, pp. 4069–4080, Aug. 2023.

[4] X. Xia, R. Xu, and J. Ma, "Secure cooperative localization for connected automated vehicles based on consensus," *IEEE Sensors J.*, vol. 23, no. 20, pp. 25061–25074, Jul. 2023.

[5] J. Li et al., "Learning for vehicle-to-vehicle cooperative perception under lossy communication," *IEEE Trans. Intell. Veh.*, vol. 8, no. 4, pp. 2650–2660, Apr. 2023.

[6] W. Liu et al., "A systematic survey of control techniques and applications in connected and automated vehicles," *IEEE Internet Things J.*, vol. 10, no. 24, pp. 21892–21916, Dec. 2023.

[7] E. W. Dijkstra, "A note on two problems in connexion with graphs," *Numerische Mathematik*, vol. 1, no. 1, pp. 269–271, 1959.

[8] P. Ferbach, "A method of progressive constraints for nonholonomic motion planning," *IEEE Trans. Robot. Autom.*, vol. 14, no. 1, pp. 172–179, Feb. 1998.

[9] S. Beyersdorfer and S. Wagner, "Novel model based path planning for multi-axle steered heavy load vehicles," in *Proc. 16th Int. IEEE Conf. Intell. Transp. Syst. (ITSC)*, 2013, pp. 424–429.

[10] D. Dolgov, S. Thrun, M. Montemerlo, and J. Diebel, "Practical search techniques in path planning for autonomous driving," in *Proc. AAAI Workshop*, 2008, pp. 1–8.

[11] S. M. LaValle and J. J. Kuffner, "Randomized kinodynamic planning," *Int. J. Robot. Res.*, vol. 20, no. 5, pp. 378–400, 2001.

[12] A. Mohamed, J. Ren, H. Lang, and M. El-Gindy, "Optimal collision free path planning for an autonomous articulated vehicle with two trailers," in *Proc. IEEE Int. Conf. Ind. Technol. (ICIT)*, 2017, pp. 860–865.

[13] J. V. Miró, A. S. White, and R. Gill, "On-line time-optimal algorithm for manipulator trajectory planning," in *Proc. Eur. Control Conf. (ECC)*, 1997, pp. 2611–2616.

[14] B. Li, Y. Zhang, T. Acarma, Q. Kong, and Y. Zhang, "Trajectory planning for a tractor with multiple trailers in extremely narrow environments: A unified approach," in *Proc. Int. Conf. Robot. Autom. (ICRA)*, 2019, pp. 8557–8562.

[15] B. Li, T. Acarman, Y. Zhang, L. Zhang, C. Yaman, and Q. Kong, "Tractor-trailer vehicle trajectory planning in narrow environments with a progressively constrained optimal control approach," *IEEE Trans. Intell. Veh.*, vol. 5, no. 3, pp. 414–425, Sep. 2020.

[16] K. Judd and T. McLain, "Spline based path planning for unmanned air vehicles," in *Proc. AIAA Guid. Navig. Control Conf. Exhibit*, 2001, pp. 73–78.
[17] T. Mercy, R. Van Parys, and G. Pipeleers, "Spline-based motion planning for autonomous guided vehicles in a dynamic environment," *IEEE Trans. Control Syst. Technol.*, vol. 26, no. 6, pp. 2182–2189, Nov. 2018.
[18] C. Ziegler and J. Adamy, "Anytime tree-based trajectory planning for urban driving," *IEEE Open J. Intell. Transp. Syst.*, vol. 4, pp. 48–57, 2023.
[19] N. Rajesh, Y. Zheng, and B. Shyrokau, "Comfort-oriented motion planning for automated vehicles using deep reinforcement learning," *IEEE Open J. Intell. Transp. Syst.*, vol. 4, pp. 348–359, 2023.
[20] R. Trauth, K. Moller, and J. Betz, "Towards safer autonomous vehicles: Occlusion-aware trajectory planning to minimize risky behavior," *IEEE Open J. Intell. Transp. Syst.*, vol. 11, pp. 1–15, 2023.
[21] M. Geisslinger, R. Trauth, G. Kaljavesi, and M. Lienkamp, "Maximum acceptable risk as criterion for decision-making in autonomous vehicle trajectory planning," *IEEE Open J. Intell. Transp. Syst.*, vol. 4, pp. 570–579, 2023.
[22] X. Zhou, H. Shen, Z. Wang, H. Ahn, and J. Wang, "Driver-centric lane-keeping assistance system design: A noncertainty-equivalent neuro-adaptive control approach," *IEEE/ASME Trans. Mechatronics*, early access, Feb. 6, 2023, doi: 10.1109/TMECH.2023.3236245.
[23] H. Zheng et al., "Learning-based safe control for robot and autonomous vehicle using efficient safety certificate," *IEEE Open J. Intell. Transp. Syst.*, vol. 4, pp. 419–430, 2023.
[24] A. A. Jawahiri, "Spline-based trajectory generation for autonomous truck-trailer vehicles in low speed highway scenarios," M.S. thesis, Dept. Comput. Sci., Delft Univ. Technol., Delft, The Netherlands, 2018.
[25] J.-W. Choi and K. Huhtala, "Constrained global path optimization for articulated steering vehicles," *IEEE Trans. Veh. Technol.*, vol. 65, no. 4, pp. 1868–1879, Apr. 2016.
[26] A. Seiffer, L. Schütz, M. Frey, and F. Gauterin, "Constrained control allocation improving fault tolerance of a four wheel independently driven articulated vehicle," *IEEE Open J. Intell. Transp. Syst.*, vol. 4, pp. 187–203, 2023.
[27] T. Thakkar and A. Sinha, "Motion planning for tractor-trailer system," in *Proc. 7th Indian Control Conf. (ICC)*, 2021, pp. 93–98.
[28] O. Ljungqvist, N. Evestedt, D. Axehill, M. Cirillo, and H. Pettersson, "A path planning and path-following control framework for a general 2-trailer with a car-like tractor," *J. Field Robot.*, vol. 36, no. 8, pp. 1345–1377, 2019.
[29] N. Evestedt, O. Ljungqvist, and D. Axehill, "Motion planning for a reversing general 2-trailer configuration using closed-loop RRT," in *Proc. IEEE/RSJ Int. Conf. Intell. Robots Syst. (IROS)*, 2016, pp. 3690–3697.
[30] H. Olov, "Motion planning for a reversing full-scale truck and trailer system," M.S. thesis, Dept. Comput. Sci., Linköping Univ., Linköping, Sweden, 2016.
[31] J. Leonard et al., "A perception-driven autonomous urban vehicle," *J. Field Robot.*, vol. 25, no. 10, pp. 727–774, 2008.
[32] O. Arslan, K. Berntorp, and P. Tsiotras, "Sampling-based algorithms for optimal motion planning using closed-loop prediction," in *Proc. IEEE Int. Conf. Robot. Autom. (ICRA)*, 2017, pp. 4991–4996.
[33] S. G. Loizou, H. G. Tanner, V. Kumar, and K. J. Kyriakopoulos, "Closed loop motion planning and control for mobile robots in uncertain environments," in *Proc. 42nd IEEE Int. Conf. Decis. Control*, vol. 3, 2003, pp. 2926–2931.
[34] F. Ghilardelli, G. Lini, and A. Piazzi, "Path generation using $\eta 4$-splines for a truck and trailer vehicle," *IEEE Trans. Autom. Sci. Eng.*, vol. 11, no. 1, pp. 187–203, Jan. 2014.
[35] K. Bergman, O. Ljungqvist, and D. Axehill, "Improved path planning by tightly combining lattice-based path planning and optimal control," *IEEE Trans. Intell. Veh.*, vol. 6, no. 1, pp. 57–66, Mar. 2021.
[36] R. Oliveira, O. Ljungqvist, P. F. Lima, and B. Wahlberg, "Optimization-based on-road path planning for articulated vehicles," *IFAC PapersOnLine*, vol. 53, no. 2, pp. 15572–15579, 2020.
[37] R. Oliveira, O. Ljungqvist, P. F. Lima, and B. Wahlberg, "A geometric approach to on-road motion planning for long and multi-body heavy-duty vehicles," in *Proc. IEEE Intell. Veh. Symp. (IV)*, 2020, pp. 999–1006.
[38] B. Li, T. Acarman, X. Peng, Y. Zhang, X. Bian, and Q. Kong, "Maneuver planning for automatic parking with safe travel corridors: A numerical optimal control approach," in *Proc. Eur. Control Conf. (ECC)*, 2020, pp. 1993–1998.
[39] B. Li, L. Li, T. Acarman, Z. Shao, and M. Yue, "Optimization-based maneuver planning for a tractor-trailer vehicle in a curvy tunnel: A weak reliance on sampling and search," *IEEE Robot. Autom. Lett.*, vol. 7, no. 2, pp. 706–713, Apr. 2022.
[40] H. Cen, B. Li, T. Acarman, Y. Zhang, Y. Ouyang, and Y. Dong, "Optimization-based maneuver planning for a tractor-trailer vehicle in complex environments using safe travel corridors," in *Proc. IEEE Intell. Veh. Symp. (IV)*, 2021, pp. 974–979.
[41] C. Altafini, "Some properties of the general *n*-trailer," *Int. J. Control*, vol. 74, no. 4, pp. 409–424, 2001.
[42] J. Park and H. J. Kim, "Online trajectory planning for multiple quadrotors in dynamic environments using relative safe flight corridor," *IEEE Robot. Autom. Lett.*, vol. 6, no. 2, pp. 659–666, Apr. 2021.
[43] S. Liu et al., "Planning dynamically feasible trajectories for quadrotors using safe flight corridors in 3-D complex environments," *IEEE Robot. Autom. Lett.*, vol. 2, no. 3, pp. 1688–1695, Jul. 2017.
[44] L. Guevara, M. Torres-Torriti, and F. A. Cheein, "Collision-free navigation of N-trailer vehicles with motion constraints," in *Proc. 12th Int. Workshop Robot Motion Control (RoMoCo)*, 2019, pp. 118–123.
[45] P. Lima, "Optimization-based motion planning and model predictive control for autonomous driving: With experimental evaluation on a heavy-duty construction truck," Ph.D. dissertation, Dept. Comput. Sci., KTH Roy. Inst. Technol., Stockholm, Sweden, 2018.
[46] M. M. Michałek, "Motion control with minimization of a boundary off-track for non-standard N-trailers along forward-followed paths," in *Proc. IEEE Int. Conf. Autom. Sci. Eng. (CASE)*, 2015, pp. 1564–1569.
[47] H. G. Bock and K. J. Plitt, "A multiple shooting algorithm for direct solution of optimal control problems," *IFAC Proc. Vol.*, vol. 17, no. 2, pp. 1603–1608, 1984.
[48] A. Wächter and L. T. Biegler, "On the implementation of an interior-point filter line-search algorithm for large-scale nonlinear programming," *Math. Program.*, vol. 106, no. 1, pp. 25–57, 2006.

HANYANG ZHUANG (Member, IEEE) received the Ph.D. degree from Shanghai Jiao Tong University, Shanghai, China, in 2018, where he is currently an Assistant Research Professor implementing research works related to intelligent vehicles. His research focus is on self-driving system development, vehicle control, and cooperative driving systems.

QIYUE SHEN received the M.S. degree in control science and engineering from Shanghai Jiao Tong University, Shanghai, China, in 2022. His research interests include motion planning and control of autonomous driving vehicles.

YEQIANG QIAN (Member, IEEE) received the Ph.D. degree in control science and engineering from Shanghai Jiao Tong University, Shanghai, China, in 2020, where he is currently a Postdoctoral Fellow with the University of Michigan-Shanghai Jiao Tong University Joint Institute. His main research interests include computer vision, pattern recognition, machine learning, and their applications in intelligent transportation systems.

WEI YUAN (Member, IEEE) received the master's degree in automation from Shanghai Jiao Tong University, Shanghai, China, in 2017, where he is currently pursuing the Ph.D. degree in control science and engineering. His main fields of interest are autonomous driving system, computer vision, deep learning, and vehicle control. His current research activities include end-to-end learning-based vehicle control and decision-making.

CHUNXIANG WANG (Member, IEEE) received the Ph.D. degree in mechanical engineering from the Harbin Institute of Technology, China, in 1999. She is currently an Associate Professor with the Department of Automation, Shanghai Jiao Tong University, Shanghai, China. She has been working in the field of intelligent vehicles for more than ten years and participated in several related research projects, such as European CyberC3 Project and ITER Transfer Cask Project.

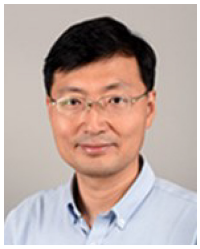

MING YANG (Member, IEEE) received the master's and Ph.D. degrees from Tsinghua University, Beijing, China, in 1999 and 2003, respectively. He is currently a Full Tenure Professor with Shanghai Jiao Tong University, the Director of the Department of Automation, and the Deputy Director of the Innovation Center of Intelligent Connected Vehicles. He has been working in the field of intelligent vehicles for more than 20 years. He participated in several related research projects, such as the THMR-V Project (first intelligent vehicle in China), European CyberCars and CyberMove Projects, CyberC3 Project, CyberCars-2 Project, ITER Transfer Cask Project, and AGV.